Electrical Transport Mechanism in $Al/V_2O_5/Al$ Microdevices

C.V. Ramana[1], B. Srinivasulu Naidu[1], O.M. Hussain[1] and C. Julien[2]
[1]Thin Film Laboratory, Department of Physics
Sri Venkateswara University, Tirupati 517 502, India
[2]Laboratoire des Milieux Désordonnés et Hétérogènes, UMR-CNRS 7603
Universite Pierre et Marie Curie, 4 place Jussieu, 75252 Paris cedex 05, France

Abstract. The current-voltage characteristics of metal-insulator-metal microdevices fabricated with electron-beam evaporated vanadium pentoxide films have been studied in order to understand the electrical transport mechanism in these films. The dependence of transport properties on various factors such as film thickness, substrate temperature, and applied field, has been established. The results revealed that the electrical transport follows a Schottky-type mechanism at lower electrical fields and a Poole-Frenkel-type at higher electrical fields than $2x10^6$ V/m.

1. Introduction

Thin films of transition-metal oxide materials with good electrical and dielectric properties find application in various electronic and optical devices [1]. The vanadium oxide system exhibits interesting electronic and optical properties because of the various valence states of vanadium cations [2-3]. Among the family of vanadium oxides, the most stable compound with the highest oxygen concentration is vanadium pentoxide (V_2O_5), which has high potential for application in the fields of microelectronics, solid-state ionics, optoelectronics, etc. [2-5]. Attention towards vanadium pentoxide in thin film form has increased in recent years because of the possibility of integration into microelectronics circuitry and by virtue of its memory switching effect, lithium ion storage capacity, and electrochromic properties [5-8].

On evaporation in vacuum, vanadium pentoxide forms non-stoichiometric V_2O_{5-x} films with oxygen deficiency, where x is a small fraction ($x \leq 0.1$). In these films a part of the V^{5+} ions is reduced to a lower oxidation state, mostly as V^{4+} ions, which have the $3d^1$ configuration [9]. It has been reported [10] that the formation of V^{4+} ions as a consequence of oxygen vacancies is quite usual even in bulk materials due to the highly polar character of vanadium pentoxide and vanadium ions in different valence states yield semiconducting properties due to the hopping process of unpaired 3d electrons from V^{4+} ions to V^{5+} ions. The partial dissociation of V_2O_5 upon evaporation in vacuum suggests that the properties as well as the particular applications of V_2O_5 thin films are mainly dependent on the deposition technique used to grow the films and the deposition conditions such deposition rate, nature of the substrate, substrate temperature, oxygen partial pressure, etc. [11]. In lithium rechargeable microbatteries, a positive electrode V_2O_5 thin film is the active material which could be associated with a film of aluminium acting as a current collector. Since the V_2O_5-Al interface plays obviously an important role, it is key to understanding this structure to have a good control of the heterojunction in the temperature range of the battery operation.

In the present work, we have investigated the metal-insulator-metal (MIM) sandwich structure prepared by the electron-beam evaporation technique using a V_2O_5 thin-film as active material. An attempt has been made to understand the electrical transport properties of this MIM structure. Results of the investigations on the electrical transport properties in $Al/V_2O_5/Al$ microdevices and their dependence on the film thickness, substrate temperature, and the applied field along with a discussion of the results are presented in this paper.

2. Experimental Technique

Thin films of vanadium pentoxide were prepared by the electron beam evaporation technique using a Balzers BA 510E high vacuum coating unit [9]. The electron beam source and the substrate distance maintained was 20 cm. The deposition of V_2O_5 thin films with thicknesses in the range from 60 to 600 nm was done onto chemically, ultrasonically and glow discharge cleaned Corning 7059 glass substrates maintained at T_s = 423 K in a vacuum of ~ $5x10^{-5}$ Pa. The deposition rate controlled by a quartz crystal thickness monitor was 3 nm/sec. The Al/V_2O_5/Al MIM microdevices were prepared by a sequential evaporation procedure in order to perform current-voltage measurements. The Al was resistively evaporated onto Corning 7059 glass substrates maintained at T_s = 423 K to serve as the bottom electrode having a width of 0.3 cm. Vanadium pentoxide film of the desired thickness was then deposited. A second Al film (0.4 cm wide) was evaporated to form the top electrode. The resulting MIM microdevice has a capacitive configuration of an effective area of 0.12 cm^2. Electrical measurements were performed on Al/V_2O_5/Al microdevices kept in a jig evacuated to ~ 10^{-2} Pa using a pA meter/dc voltage source (model Hewlett-Packard 4140B). The current-voltage characteristics were studied in the temperature range 303-403 K which is also the range of Li//V_2O_5 microbatteries operation.

3. Results

The electron-beam evaporated vanadium pentoxide thin films were uniform and the color of freshly prepared films was yellow, which indicates a good stoichiometry of the materials. The films were pin-hole free and well adherent to the substrate surface. Film composition analysis by X-ray photoelectron spectroscopy revealed that the films were nearly stoichiometric [9]. Structural investigations by X-ray diffraction and scanning electron microscopy have showed the amorphous nature of the V_2O_5 thin films [12-13]. Figure 1 shows the typical FTIR and Raman spectra of electron-beam evaporated vanadium pentoxide films grown with an amorphous structure. These results suggested that the short-range order exhibits quite similar features to that of bulk V_2O_5 with a slight modification of internal modes. The general shift of the observed stretching frequencies suggests some changes in the vanadium-oxygen bonds. The indication for the structural quality of the films is the peak position of the infrared vanadyl mode located at 1012 cm^{-1} and the Raman active mode at 993

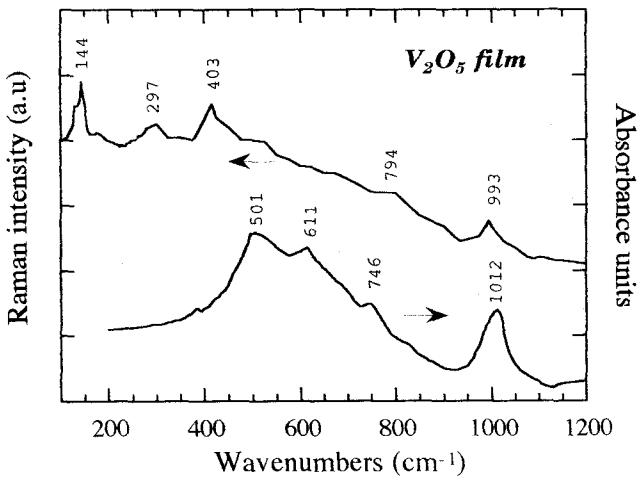

Fig. 1. FTIR and Raman spectra showing the amorphous nature of the V_2O_5 film grown on Si substrate maintained at T_s = 423 K.

cm^{-1}. The frequency shift of the vanadyl mode could be attributed to the weakening of the V=O bonding and variations in the bond length. The Raman peak at about 144 cm^{-1} in the low-frequency region is a rigid layer-like mode. The presence of this band is a clue for the layer-like structure of V_2O_5 films. The optical bandgap measured by optical absorption studies was found to be 2.3 eV [13].

3.1. Thickness Dependence of Current-Voltage Characteristics. The variation of the magnitude of the current

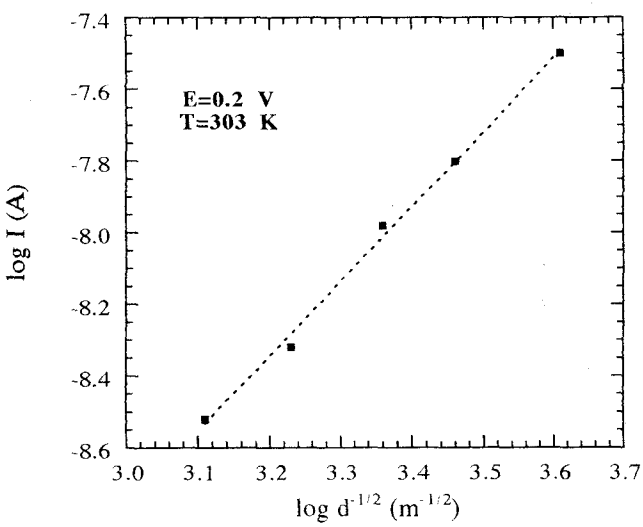

Fig. 2.Variation of the current with the inverse square root of V_2O_5 thickness, $d^{-1/2}$.

with V_2O_5 film thickness was studied to analyse the conduction mechanism in $Al/V_2O_5/Al$ microdevices. When the voltage and temperature are maintained constant, the thickness dependence of current exhibits a non-linear behavior. The increasing current observed with the increase in V_2O_5 film thickness d exhibits features shown in Fig. 2 where the current passing throughout the MIM microdevice is a function of $d^{-1/2}$. It was found that the experimental data gave a linear fit when the current was plotted against $d^{-1/2}$ at a constant voltage and temperature. Figure 3 shows the room-temperature current-voltage characteristics of $Al/V_2O_5/Al$ microdevices for various V_2O_5 film thicknesses. It is seen that the semi-logarithmic plots are almost linear with a decreasing slope when raising the V_2O_5 film thicknesses. The straight line behavior could be explained either on the basis of the Schottky emission at the electrodes or the Poole-Frenkel bulk mechanism [14-15]. In both cases the current obeys the relation of the form

$$I \propto \exp(\beta V^{1/2}/k_B T), \quad (1)$$

with the field lowering coefficient

$$\beta = (e^3/\pi\varepsilon\varepsilon_0)^{1/2}. \quad (2)$$

In these expressions V is the applied voltage, ε_0 the permittivity of free space, ε the dielectric constant of the film, k_B the Boltzmann constant, e the electronic charge and T the absolute temperature. The field lowering coefficient β can be evaluated from the rate of change of current through the $Al/V_2O_5/Al$ microdevice with the applied voltage. The field lowering coefficient β_{exp} is obtained from the slope of the linear curve of the $I\text{-}V^{1/2}$ plot. The values of β_{exp} obtained from the slopes of the linear plots are shown in Fig. 4 for various thicknesses of

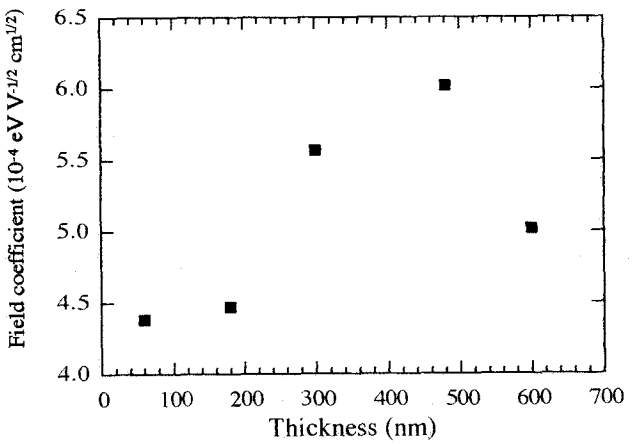

Fig. 4. Field lowering coefficients of $Al/V_2O_5/Al$ microdevices as a function of the V_2O_5 film thickness.

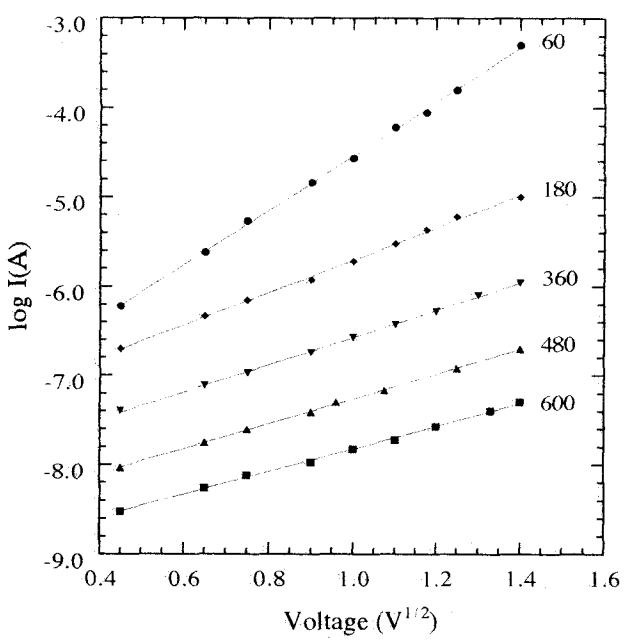

Fig. 3. The room temperature current-voltage characteristics of $Al/V_2O_5/Al$ microdevices as a function of V_2O_5 film thickness.

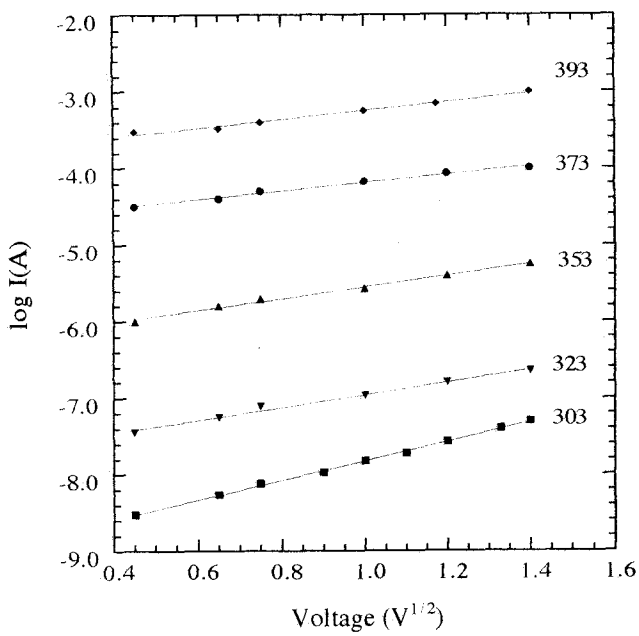

Fig. 5. Plot of log I vs. $V^{1/2}$ for $Al/V_2O_5/Al$ microdevices as a function of the temperature.

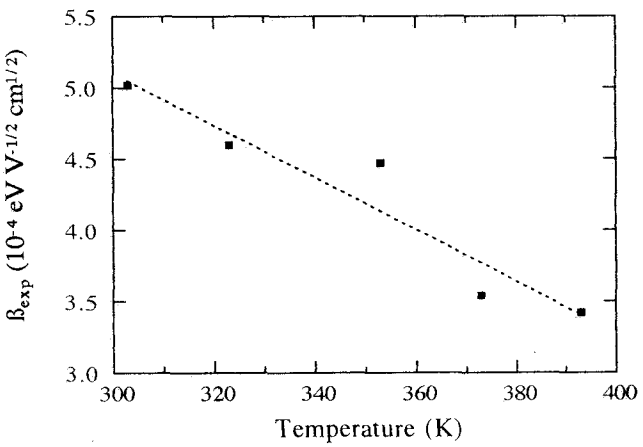

Fig. 6. Field lowering coefficients of $Al/V_2O_5/Al$ microdevices as a function of the temperature.

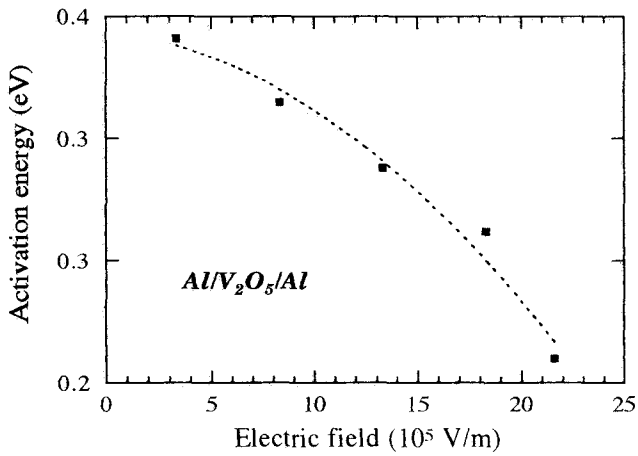

Fig. 8. Activation energy as a function of the applied electric field in $Al/V_2O_5/Al$ microdevices.

the vanadium pentoxide films. Comparing the experimental values with the theoretical ones obtained from eq. (2) using the dielectric constant given in Ref. 16, it was observed that the ratio β_{exp}/β_{th} is close to unity.

3.2. Temperature Dependence of Current-Voltage Characteristics. To have a better insight into the exact type of conduction mechanism operative in the electron-beam evaporated V_2O_5 thin films, the current-voltage (I-V) measurements were made on the $Al/V_2O_5/Al$ sandwich structure for a V_2O_5 film with a thickness of 600 nm at different temperatures. Figure 5 shows the I-V characteristics of $Al/V_2O_5/Al$ microdevices at different temperatures. It is clearly seen from this graph that the data give a linear fit when the current was plotted against $V^{1/2}$. Further, the slope of the plots decreased with the increase in temperature. The field lowering coefficients β_{exp} evaluated from the slopes of the plots at various temperatures are shown in Fig. 6. A comparison of the experimental and theoretical values indicated that the ratio β_{exp}/β_{th} is close to unity. Figure 7 shows the plots of log (I/T^2) vs. 1/T for different applied bias voltages. The plots are also found to be linear following eq. (1) for an applied bias voltage ≤ 1.3 V. Thermal activation energies evaluated from the slopes of current against inverse temperature curves are in the range 0.34-0.21 eV for the applied bias voltages in the range 0.2-1.3 V. The electric field dependence of the thermal activation energy E_a is shown in Fig. 8. It was observed that the activation energy is slightly dependent on the applied field and decreased with the increase in electric field. Therefore, the Schottky type mechanism may be operative in $Al/V_2O_5/Al$ microdevices at fields lower than $2x10^6$ V/m.

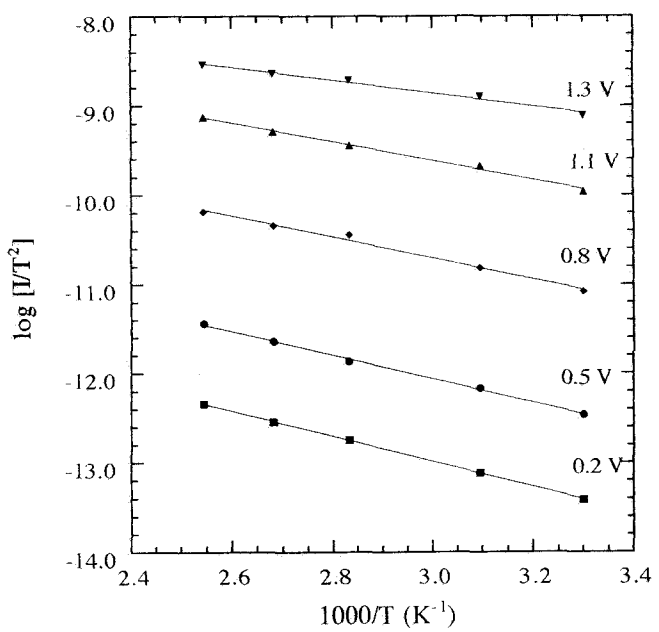

Fig. 7. Plot of log (I/T^2) vs. $10^3/T$ for $Al/V_2O_5/Al$ microdevices at different bias voltages.

4. Discussion

The conduction mechanism in an insulator/semiconductor thin film is rather complex due to the presence of defects, auto-doping centres, faults, impurities, trapping centres,

etc. in addition to the effect of work function and particularly at extremely high fields (>10^5 V/m) even with the application of a few volts across the two-potential leads. The electrical transport in a system such as metal/insulator/metal can take place by several mechanisms, e.g. as tunneling, Schottky emission, Poole-Frenkel effect, field emission and space charge limited conduction (SCLC). The mechanisms considered generally fall into two classes: thermal emission and tunneling. They divide further into bulk controlled and electrode controlled phenomena. The electrical conduction by tunneling mechanism in Al/V_2O_5/Al microdevices is eliminated from our consideration since tunneling occurs for very thin films with thicknesses in the range 5-10 nm [17]. In the present investigation, the thickness of the electron-beam evaporated vanadium pentoxide thin films is in the range 60-600 nm and hence the electron tunneling across the interfacial potential barrier could be discarded here. Further, the non-linear variation of current with V_2O_5 film thickness at a constant voltage and temperature (Fig. 2) suggests that the possibility of space charge limited current conduction in Al/V_2O_5/Al microdevices is also ruled out since the theory of space charge limited conduction mechanism predicts a linear variation of current with film thickness at a constant voltage and temperature [18]. The linear fit of the data when the current is plotted against the inverse square root of V_2O_5 film thickness indicates the possibility of current by the electrode limited process. The linear variation of the I-$V^{1/2}$ plots (Fig. 3) for various V_2O_5 film thicknesses suggests that the carrier transport in Al/V_2O_5/Al microdevices could be due to either Schottky or Poole-Frenkel mechanism. In the Schottky emission process, the electrons are emitted from the metal electrodes into the conduction band of the insulating film over the image force interfacial barrier under lowering of the applied electric field. In the Poole-Frenkel mechanism, the conduction is limited by the field-enhanced thermal emission of electrons from a discrete trap level into the conduction band. As such, the current-voltage characteristics of several insulating and semiconducting thin films can be represented by [14,15]

$$J = AT^2 \exp [(\beta_S E^{1/2} - \phi_S) / k_B T], \quad (3)$$

for the Schottky emission and

$$J = J_0 \exp (\beta_{PF} E^{1/2} - \phi_{PF}) / k_B T), \quad (4)$$

for the Poole-Frenkel emission. β_{PF} and β_S are the field lowering coefficients for the Poole-Frenkel and Schottky type conduction mechanism, respectively. ϕ_S is the metal-insulator work function for the Schottky process and ϕ_{PF} is the barrier height associated with the trap for Poole-Frenkel emission.

As shown above, both the Poole-Frenkel and Schottky effects result from the lowering of a Coulombic potential barrier by the applied electric field [19-20]. The Schottky effect is associated with the barrier at the surface of the metal and V_2O_5 film, and the Poole-Frenkel effect is associated with the barriers within the bulk of the material. The distinction between the two types of mechanism is quite difficult. Although the restoring force in both effects is due to Coulomb interaction between the escaping electron and a positive charge, they differ in that the positive image charge is fixed for the Poole-Frenkel barriers, but mobile with Schottky emission. This results in a barrier lowering twice as large for the Poole-Frenckel effect [18-19]

$$\Delta\phi_{PF} = (e^3E/\pi\varepsilon\varepsilon_0)^{1/2} = \beta_{PF} E^{1/2}, \quad (5a)$$

$$\Delta\phi_S = (e^3E/4\pi\varepsilon\varepsilon_0)^{1/2} = \beta_S E^{1/2}, \quad (5b)$$

where $\Delta\phi_{PF}$ and $\Delta\phi_S$ are the barrier lowering for Poole-Frenkel and Schottky emission, respectively.

Therefore, one can differentiate sometimes the two mechanisms by comparing the experimentally evaluated field lowering coefficient (β_{exp}) with the theoretical value (β_{th}). For Schottky emission, β_{exp} will close to β_{th} whereas for Poole-Frenkel emission, $\beta_{exp}=2\beta_{th}$. From Table 1 it is

Table 1. Experimental values of field lowering coefficients of Al/V_2O_5/Al microdevices as a function of film thickness and temperature.

Parameters		β_{exp} (eV $V^{-1/2}$ $cm^{1/2}$)	β_{exp}/β_{th}
∂ (nm)	60	4.38×10^{-4}	1.06
	180	4.47×10^{-4}	1.08
	300	5.57×10^{-4}	1.35
	480	6.02×10^{-4}	1.46
	600	5.02×10^{-4}	1.21
T (K)	303	5.02×10^{-4}	1.21
	323	4.60×10^{-4}	1.11
	353	4.47×10^{-4}	1.08
	373	3.54×10^{-4}	0.85
	393	3.42×10^{-4}	0.83

evident that the ratio β_{exp}/β_{th} is close to unity with a slight deviation with the increase in V_2O_5 film thickness. Therefore, the Schottky type mechanism may be operative in $Al/V_2O_5/Al$ microdevices. However, as pointed out by Mead [21], a linear relationship of log I vs. $V^{1/2}$ does not necessarily imply the Schottky effect but a convincing evidence of the effect. Further, several authors have reported [18-20] the Poole-Frenkel emission in thin insulating oxide films even though the experimental field lowering coefficients are compatible with the Schottky coefficient. In addition, the extrapolation of the linear plots for a common barrier and for various film thicknesses should pass through a single point at V = 0 in the case of Schottky emission, which was not observed in the present case. Also, a plot of log (I/T^2) versus $10^3/T$ should be a straight line at a fixed bias voltage according to eq. (4). Hence the exact demarcation between the two types of mechanisms is less clear at this stage.

The current-voltage characteristics of the electron beam evaporated V_2O_5 thin films (600 nm thick) at different temperatures were studied in order to understand the exact conduction mechanism. The experimental data showed a better linear fit for I vs. $V^{1/2}$. Further it is seen from Table 1 that the experimentally evaluated field lowering coefficients are very close to the theoretical value and their ratio is almost unity. At low applied voltages, an ionic component of the charge is built up from the oxygen vacancies present in the bulk of the V_2O_5 film, which enhances the field at the injecting electrode leading to a rapid rise in current. But as the applied field is increased, at some particular voltage, electrons emitted from the electrodes are trapped in the bulk of the V_2O_5 film, thereby reducing the ionic component of charge and lowering the field near the injecting electrode. Hence the current increases steadily and linearly with $V^{1/2}$. A linear behaviour is observed in the current-temperature characteristics at different applied bias voltages. Also, the data are found to give the linear fit when $\log(I/T^2)$ was plotted against (1/T) as predicted by eqn. (3) for the Schottky mechanism. These observations led to the idea that the transport properties in $Al/V_2O_5/Al$ microdevices could be dominated by the Schottky process. Thus the current-voltage characteristics of electron-beam evaporated vanadium pentoxide films and their dependence on film thickness, applied electric field, temperature, nature of electrodes and polarity of the electrodes were found to be exhibiting the quite accurate general behavior as predicted by the Schottky process.

Therefore it is concluded that the electrical transport conduction mechanism in electron-beam evaporated vanadium pentoxide thin films is of Schottky type.

Based on these results, the conductivity of electron-beam evaporated vanadium pentoxide thin films may be explained as follows. The conductivity in sub-stoichiometric vanadium oxide is believed to have two components, electronic and ionic. The ionic conduction is characterized by low mobilities while the electronic conduction is associated with relatively high mobilities. It is not possible to give a definite limit to the activation energy. As a general rule [22], activation energies lower than 0.2 eV might be considered as indicating undoubtedly electronic conduction mechanisms and activation energies in excess of 0.6 eV would be often associated with the ion transport. However, these distinctions are remarkable in crystalline materials where electrons may be expected to have high mobilities and the observed activation energies correspond either to donor and acceptor ionization or variation of mobility with temperature in the case of space-charge limited current flow. But in amorphous materials the mobility is very low, so the conduction is by hopping between localized states. Jonscher [23] proposed a model on the basis of which the amorphous materials conduct electricity by means of electron motion either in the localized levels (hopping) or in free bands. In the present case, the activation energies evaluated from the slopes of the I vs. (1/T) plots are in the range 0.34-0.21 eV for the applied bias voltages in the range 0.2-1.3 V. Further it is evident from Fig. 8 that the conduction mechanism in electron beam evaporated vanadium pentoxide thin films is a thermally activated process. A similar type of thermally activated process of conduction mechanism was also observed in vanadium pentoxide thin films prepared by thermal evaporation [24] and also in other insulating oxide thin films. It is observed that the activation energy is slightly dependent on the applied field and its value decreased slowly with increase in the applied electric field. The functional dependence of conductivity on temperature of amorphous vanadium pentoxide thin films may be explained as follows. Sub-stoichiometric vanadium pentoxide thin films contain oxygen vacancies. Oxygen vacancies capable of capturing one or two electrons act as donors in which one electron may be ionized thermally and the other one optically. The mobility of these donors is generally low and becomes high only at high temperatures. The increase in current through $Al/V_2O_5/Al$ micro-

devices with increase in temperature may be ascribed to a slight increase in the mobility of these donors. As the mobility of donors becomes high, the electronic part of conuction dominates the ionic part. When a dc voltage is applied, the positive effective charges (oxygen vacancies) move continuously towards the negative electrode. The increase in the positive charge near the negative electrode results in the positive space charge and in the remaining thickness of the material there is a negative space charge of electrons. The remaining oxygen vacancies in the bulk of the material are surrounded by electrons in excess of equilibrium density and therefore the probability of a vacancy being ionized and travelling to the negative electrode is small. This results in the saturation of current-voltage curves.

5. Conclusion

The electrical transport properties of Al/V_2O_5/Al sandwich structures of electron-beam evaporated vanadium pentoxide thin films 60-600 nm thick were studied. The linear dependences of the current on the inverse square root of oxide film thickness at a constant voltage and also on the square root of the applied voltage for various film thicknesses suggest either the Schottky of Poole-Frenkel mechanism responsible for the electrical transport in Al/V_2O_5/Al microdevices. The detailed investigations on Al/ V_2O_5/Al microdevices of V_2O_5 film of a thickness of 600 nm at various temperatures and applied bias voltages also revealed the Schottky conduction mechanism. The current-voltage characteristics of electron-beam evaporated V_2O_5 films and their dependence on thickness, applied electric field, and temperature were found to be exhibiting the quite accurate general behavior as predicted by the Schottky process and strongly suggests that the electrical transport conduction mechanism in these vanadium pentoxide thin films is of Schottky type at fields lower than $2x10^6$ V/m. The thermal activation energies obtained in the temperature range 303-393 K were 0.32-0.21 eV for the applied bias voltage in the range 0.2-1.3 V. The increase in the current through Al/V_2O_5/Al microdevices with increasing temperature may be due to the mobility of donors formed as a result of oxygen vacancies.

6. Acknowledgements

One of the author (C.V.R) is thankful to the Council of Scientific and Industrial Research (CSIR), New Delhi, India for providing Research Associateship.

7. References

[1] N. Tsuda, K. Nasu, A. Yanase and K. Siratori, Electronic Conduction in Oxides, Springer series in Solid State Sciences 94 (1991).

[2] J.C. Parker, D.J. Lam, Y.N. Xu and W.Y. Ching, Phys. Rev. B **42**, 5289 (1990).

[3] G. Micocci, A. Serra, A. Tepore, S. Capone, R. Rella and P. Siciliano, J. Vac. Sci. Tech. **15**, 34 (1997).

[4] S.F. Cogan, N.M. Nuguyen, S.T. Perrotti and R.D. Raugh, Proc. Soc. Photo-Opt. Instrum. Eng. **57-62**, 1016 (1988).

[5] A. Telledo and C.G. Granqvist, J. Appl. Phys. **77**, 4655 (1995).

[6] G.S. Nadkarni and V.S. Sirodkar, Thin Solid Films **105**, 115 (1983).

[7] C. Julien and G.A. Nazri, Solid State Batteries: Materials Design and Optimization, Kluwer, Boston, 1994.

[8] A. Telledo, A.M. Anderson and C.G. Granqvist, J. Mater. Res. **5**, 1253 (1990).

[9] C.V. Ramana, O.M. Hussain, B. Srinivasulu Naidu and P.J. Reddy, Thin Solid Films **305**, 219 (1997).

[10] L. Rivoalen, A. Revcolevschi, J. Livage and R. Collongues, J. Non-Cryst. Solids **21**, 171 (1976).

[11] L.I. Maissel and R. Glang, Hand Book of Thin Film Technology, Mc-Graw Hill, New York, 1970.

[12] C.V. Ramana, O.M. Hussain, B. Srinivasulu Naidu and PJ. Reddy, Vacuum **48**, 431 (1997).

[13] C.V. Ramana, O.M. Hussain, and B. Srinivasulu Naidu, Mat. Chem. Phys. **50**, 195 (1997).

[14] G. Langyel, J. Appl. Phys. **37**, 807 (1966).

[15] J. Frenkel, Phys. Rev. **54**, 647 (1938).

[16] C.V. Ramana, O.M. Hussain, B. Srinivasulu Naidu and C. Julien, Mat. Sci. Eng. B **60**, 173 (1999).

[17] J.G. Simmons, in: Handbook of Thin Film Technology (L.I. Maissel and R. Glang, eds.) Mc-Graw Hill, New York, 1970, chapter 14.

[18] M. Kryszenski and A. Sdzymanski, Macromol. Rev. **4**, 245 (1970).

[19] C.A. Mead, Phys. Rev. **128**, 2088 (1962).

[20] P. Mark and E. Hartman, J. Appl. Phys. **39**, 2163 (1968).

[21] C.A. Mead, in: Basic Problems in Thin Film Physics (R. Niedermayer and H. Mayer, Eds.) Vandenhoeck and Ruprecht, Goettingen, 1960.
[22] M. Anwar and C.A. Hogarth, Int. J. Electronics **66**, 419 (1989).
[23] A.K. Jonscher, J. Vac. Sci. Technol. **8**, 135 (1971).
[24] V.S. Pankajakshan, K. Neelakandan and M.C. Lancaster, Thin Solid Films **251**, 196 (1992).

Manuscript rec. May 15. 2000; acc. Dec. 12, 2000.